



Citation for published version:

Barbosa, AI, Edwards, AD & Reis, NM 2021, 'Antibody Surface Coverage Drives Matrix Interference in Microfluidic Capillary Immunoassays', *ACS Sensors*, vol. 6, no. 7, pp. 2682-2690.
<https://doi.org/10.1021/acssensors.1c00704>

DOI:

[10.1021/acssensors.1c00704](https://doi.org/10.1021/acssensors.1c00704)

Publication date:

2021

Document Version

Peer reviewed version

[Link to publication](#)

© ACM, 2021. This is the author's version of the work. It is posted here by permission of ACM for your personal use. Not for redistribution. The definitive version was published in *ACS Sens*, {VOL#,6 ISS# 7, (17/06/2021)}
<https://pubs.acs.org/doi/10.1021/acssensors.1c00704>

University of Bath

Alternative formats

If you require this document in an alternative format, please contact:
openaccess@bath.ac.uk

General rights

Copyright and moral rights for the publications made accessible in the public portal are retained by the authors and/or other copyright owners and it is a condition of accessing publications that users recognise and abide by the legal requirements associated with these rights.

Take down policy

If you believe that this document breaches copyright please contact us providing details, and we will remove access to the work immediately and investigate your claim.

Antibody surface coverage drives matrix interference in microfluidic capillary immunoassays

Ana I. Barbosa^{†,#}, Alexander D. Edwards^{§,#}, and Nuno M. Reis^{‡,#,*}

[†]Department of Chemical Engineering, Loughborough University, Loughborough, LE11 3TU, United Kingdom, [#]Capillary Film Technology Ltd, Daux Road, Billingshurst, RH14 9SJ West Sussex, United Kingdom, [§]Reading School of Pharmacy, University of Reading, Whiteknights, Reading RG6 6AD, United Kingdom, [‡]Department of Chemical Engineering and Centre for Biosensors, Bioelectronics and Biodevices (C3Bio), University of Bath, Claverton Down, Bath BA2 7AY, United Kingdom

Abstract

The performance of biosensors is often optimised in buffers, which brings inconsistencies during applications with biological samples. Current strategies for minimising sample (matrix) interference are complex to automate and miniaturise, involving e.g. sample dilution or recovery of serum/plasma. This study shows the first systematic study using hundreds of actual microfluidic immunoassay fluoropolymer strips to understand matrix interference in microflow systems. As many interfering factors are assay-specific, we have explored matrix interference for a range of enzymatic immunoassays, including a direct mIgG/anti-mIgG, a sandwich cancer biomarker PSA and a sandwich inflammatory cytokine IL-1 β . Serum matrix interference was significantly affected by capillary antibody surface coverage, suggesting for the first time the main cause of serum matrix effect is low-affinity serum components (e.g. auto-antibodies) competing with high-affinity antigen for the immobilised antibody. Additional experiments carried out with different capillary diameters confirmed the importance of antibody surface coverage in managing matrix interference. Building on these findings we propose a novel analytical approach where antibody surface coverage and sample incubation times are key for eliminating and/or minimising serum matrix interference, consisting in bioassay optimization carried out in serum instead of buffer, without compromising the performance of the bioassay nor adding extra cost nor steps. This will help establishing a new route towards faster development of modern point-of-care tests and effective biosensors development.

Keywords: Matrix effect; Microfluidics; Biosensors; Protein Biomarkers; Microcapillary Film.

* **Corresponding author:** N. M. Reis. E-mail: n.m.reis@bath.ac.uk; Tel.: +44(0)1225 383 369.

Components of biological samples are known to interfere with the performance of diagnostics tests, by affecting the response of the test to the analyte of interest.¹ This has a direct impact on sensitivity, specificity, and variability of the test leading to inaccurate analyte quantitation in real biological samples.^{2,3} According to current literature, this called matrix interference or effect can be caused by different components, such as blood cells, sample viscosity, or plasma components such as heterophilic antibodies (antibodies produced against poorly defined antigens presenting low affinity and weak binding),⁴ human anti-animal antibodies (HAAA, high affinity antibodies generated when the immune system is in contact with animal antibodies),⁵ and other plasma proteins such as albumin, lysozyme, fibrogen and paraprotein have reported tests interferences.⁶ *Boscato et al.* (1986) showed that analyte-antibody binding substances were detected in 40% of studied samples (688 samples), being responsible for 15% interference in assays.⁷ Appropriate matrix management is therefore essential to develop reliable bioassays and biosensors, however this is very dependent on the molecular analysis platform, since the type of reagents (e.g. antibody purity), and the antibody binding conditions (e.g. antibody affinity, diffusion distance, surfaces interactions) are key contributors to matrix effect. Although current procedures for dealing with matrix interference can be effectively implemented in a centralised pathology lab, involving conventional sample preparation methods such as dilution, centrifugation, precipitation, etc, these methods are not universal, and fail to serve sensitive and automated detection desired in automated point-of-care (POC) microfluidic platforms.⁸ Currently, little is known in literature about matrix interference in microfluidic systems which needs to be addressed in order to speed up adoption of microfluidic bioassays and biosensors.

In order to find an universal way to deal with matrix effect at POC settings, there is a plethora of microfluidic plasma separation devices aiming to eliminate sample matrix interference protein bioassays performed by novel biosensor platforms.^{9,10} However, plasma or serum still contain interfering factors which affect the accuracy of the tests.¹¹ POC analytical approaches would greatly benefit from overcoming biological matrix interference without laboratory equipment, since any sample preparation required for a POC test compromises the speed, complexity and cost of the test. Therefore, understanding the biological matrix interference and finding strategies to overcome it is a paramount for POC diagnostic industry and biosensors research,¹² that aim to combine sensitive, accurate and rapid protein quantitation with cost-effective test development, demanded by the ever-increasing biomarker use in patients' stratification and personalised medicine.^{3,8,13,14} Many biosensors are incorporated into lab-on-chip devices that test plasma or serum separated outside the micro device using centrifugation, reducing benefits of miniaturisation.¹⁵ A growing number of microfluidic strategies aim to incorporate *in situ* plasma separation from whole blood¹⁴ using microstructures,¹⁶ gravity-driven separation,¹⁷ micro-centrifugation,¹⁸ capillary-driven contactless electrophoresis,¹⁹ and plasma skimming effect sometimes referred to as the Zweifach–Fung effect.^{20,21} However, very few studies report the measurement of protein biomarkers after the blood plasma separation, which hinders the validation of the developed devices and methods for protein biomarkers quantitation.

Furthermore, the microfluidic studies that actually report protein detection in plasma,^{22,23} do not report recovery or sample variability studies, hampering the understanding of how blood or plasma sample matrix affects protein biomarker detection in microfluidic devices, and consequently how to solve sample variability effect. In fact, obtaining data that reflects how sample components affect antibody-antigen binding in a specific microfluidic device can be difficult to obtain, not only due to the variety of interference factors, but also due to the prototype nature of microfluidic devices that are not manufactured in large-scale, reducing the number of replicates need for the study. Several studies use real-time antibody-antigen detection techniques such as OWLS (Optical Waveguide Lightmode Spectroscopy), ellipsometry, or QCM (quartz crystal microbalance) that although very precise for antibody binding affinity determination, use polymer coated specific surfaces that not always replicate the surface chemistry of the actual microfluidic devices. Also, these systems do not reflect the geometry of the microfluidic devices, which can lead to errors when translating assay conditions from real-time detection techniques microfluidic systems.^{24,25}

In the present work, we explored matrix interference in microfluidic protein immunoassays using hundreds of fluorinated, Teflon FEP microfluidic strips fabricated from a melt-extruded, mass-manufactured 10-bore microcapillary film (MCF), connected to multiple syringe aspirator developed in-house (Figure 1A). Microfluidic protein bioassays presented significant variations when performed in buffer or human serum (Figure 1B), confirming matrix interference is also present in microfluidic bioassays. Based on our previous experience in carrying out high-performance immunoassays in this microfluidic platform,^{3,26} we hypothesized the actuation mechanism of the interfering factor(s) (Figure 1C) is closely related to the antibody surface coverage. Consequently, we explored the impact of antibody surface coverage on sample matrix interference for three distinct protein bioassays, as interference can be very assay-specific.^{27,28} We addition, we studied other parameters that appear to contribute to the matrix interference, with particular focus on sample incubation time and capillary diameter. We gathered the outcomes into a new bioanalytical approach for minimizing matrix interference in immunoassay protein detection.

EXPERIMENTAL SECTION

Materials & Reagents. Mouse IgG (mIgG), whole antibody was purchased from Life Technologies (Paisley,UK), rabbit anti-mIgG (whole molecule) conjugated with peroxidase and SIGMAFAST™ OPD (o-Phenylenediamine dihydrochloride) tablets were supplied from Sigma-Aldrich (Dorset, UK). The IL-1 β recombinant protein, Anti-Human IL-1 β biotin and Anti-Human IL-1 β purified were supplied from eBiosciences (Hatfield, UK). High sensitivity streptavidin-HRP was supplied by Thermo Scientific (Lutterworth, UK). Human kallikrein 3/ Prostate Specific Antigen (PSA) ELISA kit was purchased from R&D Systems (Minneapolis, USA). The kit contained a monoclonal mouse Human Kallikrein 3/PSA antibody (CapAb), a Human Kallikrein 3/PSA polyclonal biotinylated antibody (DetAb) and recombinant Human Kallikrein 3/PSA (standard). Phosphate buffered solution (PBS) and Bovine Serum Albumin (BSA) were

sourced from Sigma Aldrich (Dorset, UK). PBS pH 7.4, 10mM was used as the main experimental buffer. The blocking solutions consisted in 3% w/v protease-free BSA diluted in PBS buffer and a Super Blocking solution purchased by Thermo scientific (Lutterworth, UK). For washings, PBS with 0.05% v/v of Tween-20 (Sigma-Aldrich, Dorset, UK) was used. A female human serum was supplied from BBI solutions (Cardiff, UK), aliquot and storage at -20°C. The human blood was collected into a 5 ml vial with citrate phosphate dextrose (CPD) as anti-coagulant, supplied by healthy volunteers at Loughborough University.

Microfluidic fluoropolymer MCF strips. The micro-engineered MCF material (materials and geometry detailed in Supplementary Information, SI)^{29,30} is particularly well suited to study systematically the role of sample matrix on heterogeneous immunoassays, enabling simple and rapid manufacturing of hundreds or thousands of disposable strips in very identical condition at negligible cost, that would be hard to match with other microfluidic devices. Also, the whole inner section of the cylindrical/elliptical capillaries is homogeneously coated with the capture antibody in contrast to immobilization on a single surface as it happens for many other microfluidic devices, which offers advantages in studying surface coverage and specific/non-specific surface binding.³¹

Effect of antibody surface coverage. In order to understand how antibody surface coverage influences human serum interference in MCF protein tests, three different assays (mIgG/anti-mIgG, IL-1 β and PSA assay), presenting different analytical antibodies, were studied in 212 μ m diameter bore MCF. The antibody surface coverage of these assays was varied by loading captured antibody solutions in the range of 0 -200 μ g/ml. The antigen concentration was kept constant in the three assays, being 0.6 μ g/ml, 0.125 ng/ml and 3.75 ng/ml for anti-mIgG peroxidase conjugated, IL-1 β and PSA respectively, as well as the antigen/sample incubation time that was 5 minutes. IL-1 β and PSA assays follow same conditions as previously reported,^{3,32} and briefly described in SI. Digital images were taken of MCF strips in the three studied assays after 5 minutes of OPD enzymatic substrate loading. The described assays were performed in the exact same conditions preparing antigen solutions in buffer and in non-diluted human serum (refer to the SI document for more details).

Effect of sample incubation time. In order to better understand the sample incubation effect in the matrix interference in MCF protein assays, an IL-1 β sandwich assay³² was performed in non-diluted human serum, whole blood and buffer. Instead of full response curves, only four IL-1 β concentrations were tested (0, 0.03, 0.125 and 0.5 ng/ml). The sandwich assays were performed with 5 and 30 minutes of sample incubation. To perform the IL-1 β full response curve, a solution of 40 μ g/ml of anti-IL-1 β CapAb was used as coating solution in 212 \pm 16 μ m diameter MCF, and 1:2 serial dilutions of 0-1 ng/ml range of IL-1 β were spiked in buffer, 50% serum and 100% serum as sample diluents. The samples were incubated for 5 and 30 min. The 4-parameter logistic (4PL) mathematical model was fitted to the experimental data by the minimum square

difference for each full IL-1 β response curve. The lower limit of detection was calculated by the mean absorbance of the blank plus three times the standard deviation of the blank samples.

Effect of capillary diameter. Several transversal sections of three FEP MCFs with different capillaries diameter were trimmed and a long focal distant point microscope (Nikon SMZ 1500 stereo microscope) was used for imaging. ImageJ software was used to measure the diameter of the 10 capillaries from the microphotographs.³³ A solution of 200 $\mu\text{g/ml}$ of mIgG was filled into three different diameters (109, 212 and 375 μm) MCF strips with 35 cm length each. A negative control strip was filled with PBS buffer. The solutions were incubated for 30 minutes at room temperature and washed with 1 ml of PBS-Tween. A solution of 0.6 $\mu\text{g/ml}$ of mouse anti-mIgG peroxidase conjugated, prepared in PBS buffer, was added to the MCF strip and 4 cm strips were trimmed and washed with PBS-Tween after variable incubation times of anti-mIgG. The 1 OPD substrate (1 mg/ml) was added to the strips and digital images taken with a flatbed scanner after 5 minutes of enzymatic substrate incubation. The procedure was repeated for 0.6 $\mu\text{g/ml}$ anti-mIgG peroxidase conjugated solutions prepared in non-diluted human serum.

Kinetics of antibody-antigen binding. Equation (E1) was solved analytically for a constant analyte concentration and used to estimate the rates of association and dissociation of antibody binding in the MCF system.³⁴

$$Abs = \frac{K_{on} Abs_{max} C}{K_{on} C + K_{off}} (1 - e^{-(K_{on} C + K_{off})t}) \quad (E1)$$

where *Abs* is the optical absorbance signal correspondent to antigen surface density at the time *t*; *C* is the antigen bulk concentration; *K_{on}* the association rate and *K_{off}* the dissociation rate; *Abs_{max}* is the maximum Abs signal corresponding to the maximum antigen surface coverage.

Image analysis of the microfluidic MCF strips. RGB digital images of the immunoassay strips were split into 3 separated channels images by *Image J* software (NIH, Maryland, USA). The blue channel images were used to calculate absorbance values, based on the grey scale peak height of each individual capillary of Teflon FEP MCF as described previously.^{3,29,35} Therefore, absorbance signal is calculated for each capillary, according Beer-Lambert equation. The absorbance values presented averages of absorbance from 10 capillaries in a given MCF strip.

RESULTS AND DISCUSSION

Matrix interference is linked to antibody surface coverage. It has been previously shown that antibody surface coverage is related with immobilized antibodies functionality since it interferes with their orientation and steric hindrance.³¹ Therefore, we explored the impact of antibody monolayer on serum matrix

effect, since it would favour the binding of high affinity components – antigens. As matrix interference is usually dependent on diagnostic antibodies,⁸ we have tested three different immunoassays: a direct mouse IgG/anti-mouse IgG, a sandwich human PSA, and a sandwich human IL-1 β , covering a range of high-performance immunoassays. We manipulated the antibody surface coverage by varying the concentration of capture antibody loaded into the microcapillaries, with absorbance responses tested in both buffer and undiluted serum. Surprisingly, we noticed full agreement of optical signal between buffer and undiluted human serum for a narrow range of concentration of capture antibody (Figure 2), with the window of agreement being very immunoassay-specific.

For the mIgG/anti-mIgG immunoassay (Figure 2A), where both antibodies are polyclonal and do not present site-specific binding, larger antibody surface coverages obtained from 50–200 $\mu\text{g/ml}$ mIgG solutions fully eliminated the matrix interference in undiluted serum. Similar results were observed for IL-1 β sandwich assay, where matrix interference was fully eliminated with antibody surface coverages in the range of 40-200 $\mu\text{g/ml}$ (Figure 2B). Based on a previous FEP adsorption study,³¹ we know these CapAb concentrations promote the formation of half of antibody monolayer with antibodies oriented “end-on” with Fab regions in line, enhancing antigen capture in microcapillary bioassays. This agrees with findings in literature for a thyroxin assay, where the replacement of an antibody coverage with low affinity by high affinity eliminated the matrix effect of serum samples,³⁶ explained by the low affinity binding of the interfering factor(s) to the immobilised antibody. Consequently, higher antibody coverages with properly oriented antibodies present higher antigen binding capacity, minimising sample matrix interference. This is in line with conclusions in another study that reported matrix proteins bind non-specifically to the immobilized receptors in IL-6 and acute phase proteins (PCT) immunoassays, however not preventing the analyte binding.³⁷

The sandwich PSA (Figure 2C), where the immobilized antibody is monoclonal and the detection antibody polyclonal, showed a contrasting behaviour, with matrix interference minimised for a narrow window of concentrations (10-20 $\mu\text{g/ml}$) of capture antibody, which is significantly lower than for the other antibody systems shown in Figures 2A-B. The polyclonal anti-PSA detection antibody binds directly to the monoclonal capAb in the absence of antigen, therefore an increment in CapAb promotes a higher increment of the signal in buffer than in serum, suggesting a competition of the detAb with the interfering components from the serum.

These results mean that the narrow window for anti-PSA loading will reduce the assay sensitivity, since the sensitivity is related with higher antigen capture and that is related with higher amount of functionalised antibodies in the surface. Nevertheless, this assay presents the necessary sensitivity for its application, since PSA clinical threshold is 4 ng/ml.³ It is also important to note that optimising the capture antibody loading in buffer could lead to significant errors in terms of assay performance. In comparison the IL-1 β assay composed by two monoclonal antibodies presents higher sensitivities since the antibodies are less

prone to interference, which is coherent with general knowledge that assay performance is dependent on antibodies nature.³²

Matrix interference is time-dependent. Longer samples incubation times increase the probability of lower affinity components to be desorbed and higher affinity compounds to be bound. In line with our previous experience with PSA sandwich immunoassay,³ where we found a significant impact of sample incubation time in the matrix interference using both whole blood and serum, we have further studied the effect of sample incubation time using a monoclonal pair sandwich assay system. Therefore, we have separately fully tested the effect of sample incubation time and different sample diluents for monoclonal quantitation of IL-1 β (Figure 3). Human serum matrix interference was fully eliminated through extending the sample incubation from 5 to 30 minutes. For whole blood, matrix interference was mostly eliminated for the range of antigen concentrations tested, only with the negative control showing an increase on background signal (Figure 3A and B). This is undesirable as it impacts on the overall limit of detection, yet it can very possibly be addressed through straightforward assay development, such as optimisation of the buffer and blocking solutions.

On the overall, the response curves shown in Figures 3C and 3D agreed with previous studies with the same PSA sandwich immunoassay³ and demonstrated adequate sample incubation time needs to be combined with suitable antibody surface coverage for minimising matrix effect in microcapillary assays. These findings suggest the matrix interference is time-dependent and very probably linked to a competition for binding sites between low-affinity interfering factor(s) with high-affinity antigen and/or detection antibody/complex.

A conventional strategy for reducing sample matrix interference in high-sensitivity immunoassays involves diluting the sample, which can be effective depending on the sample dilution factor.^{37,38} Figure 3C shows for short incubation time a good overlap of full IL-1 β response curves in buffer and 50% human serum, confirming sample dilution is also effective in capillary immunoassays, agreeing with our previous results for PSA sandwich immunoassay with human serum and whole blood samples for both colorimetric and fluorescent detection.^{3,26} Yet, in respect to POC applications, sample dilution adds another complex step which requires automation and can compromise the clinical value of the test by reducing the limit of detection of the immunoassay. In the case of IL-1 β sandwich immunoassay, we noticed sample dilution resulted in similar lower limit of detection (LLoD) in 50% human serum matrix compared to 100% human serum (Table 1), therefore rapid, high-performance quantitation is also possible in capillary immunoassays upon sample dilution. Table 1 also shows longer incubation times increase LLoDs. LLoDs are determined by the blank value and its standard deviation, therefore their variation is related with the development of background noise, which can be caused by non-specific binding of serum/blood components. Therefore, although longer periods increase the probability of desorption of low-affinity components in the presence of the analyte eliminating the matrix effect, they increase the probability of non-specific binding in the absence of the analyte, negatively impacting assays LLoD. Thus is important to find the suitable sample incubation time that can provide simultaneously the management of matrix effect and maintain the desired LLoD performance.

Diameter dependence of matrix effect. We have recently reported that surface coverage of antibody by passive adsorption in Teflon FEP microfluidic strips is dependent on the capillary diameter³¹ (Figure 4A). From a theoretical perspective, the capillary diameter is known to affect the total surface area (SA) available for antibody immobilization, as well as the sample/reagent volume (V), which in turn affects the mass and density of immobilized capture antibody. On the other hand, the surface-area-to-volume (SAV) becomes an important parameter as it can govern the antigen-antibody equilibrium and rate of reaction rate, on the overall the choice about the capillary diameter can be seen as a balance between the total SA and the SAV (Figure 4B). Although surface density (ng/cm) is independent of the diameter of the capillary, due to the smaller sample volume loaded, small diameter capillaries yield a much lower surface density of immobilized antibody compared to larger diameter capillaries. In such case, the number of adsorbed molecules is limited by the number of molecules in solution. Barbosa et al³¹ reported half of the amount of immobilized antibody on the 109 μm diameter MCF compared to the amount immobilized on the 212 μm . On the other hand, the 375 μm diameter MCF also presented a significantly higher surface density compared to the 212 μm MCF (867.8 ng/cm² and 609.5 ng/cm², respectively). Capillary diameter also affects the maximum diffusion distance that molecules have to travel in a heterogeneous immunoassay (where the capture antibody is immobilised on the inner wall of the capillaries) with the time of diffusion increasing to the square of the distance according to Einstein's law of diffusion.³⁹ Diffusion can be affected by the viscosity of the sample, however immunoassay signal with serum samples were not significantly different than signal with the buffer and we have not detected any significant variations in both assay kinetics and equilibrium as show and discussed in Supplementary Information (Figure S1 and Table S1). Consequently, we have studied the effect of capillary diameter in MCF capillary assays with mIgG/anti-mIgG assay. We noticed a decrease in capillary diameter from 212 to 109 μm in buffer resulted in 2 min faster antibody-antigen equilibrium, while an increase in capillary diameter from 212 to 375 μm delayed the equilibrium in 2 min, confirming capillary immunoassays are also diffusion limited (Figure 4C and Table 2). Note that kinetic constants obtained reflect the overall strength and stability of the antibody monolayer, which depends on structural rearrangements of mouse IgG antibodies, and the fact that anti-mouse IgG can bind in bivalent way to the immobilised antibodies if properly oriented. Also, low affinity antigen, like anti-mIgG, it is strongly affected by mIgG density and therefore structural orientation.⁴⁰ Further experiments with undiluted human serum showed the equilibrium is surprisingly changed for small capillaries (Figure 4D and Table 2) in the presence biologic human serum matrix, revealing a level of interference of the matrix that could not be detected by comparing other microcapillary diameters tested. This can be explained by the different antibody surface coverages in the different capillary geometries due to the adsorption equilibrium and on/off rates of the immobilised antibody onto Teflon FEP surfaces being dependent on capillary geometry as explained previously. On the overall, this confirmed a correlation between antibody surface coverage, microcapillary diameter and matrix interference, with reduced antibody coverages being more prone to matrix interference.

Novel analytical approach for managing matrix interference in microcapillary protein immunoassays. We have combined the new finding in sample matrix interference with our several years' experience in high-performance microcapillary immunoassays to propose a new analytical approach (Figure 5A), which we believe will help the effective management of sample matrix in miniaturised immunoassays. This approach can easily be integrated in routine assay development helping to deliver more robust microfluidic immunoassays, especially in the MCF platform, enabling rapid, sensitive, accurate and decentralised quantitative protein immunoassay testing (Figure 5B). The first stage in the development of e.g. a protein sandwich immunoassay should be the choice of optimal antibody surface coverage for minimal matrix interference. This can be done by changing CapAb concentration in buffer yet it is essential this is also carried out in human serum. Low antigen concentrations will favour the antibody surface coverage yielding enhanced limit of detection for the test (Phase A, Figure 5). For best signal-to-noise ratio (yielding the lowest limit of detection), concentration and incubation times should be optimised for both detection antibody and enzyme. This assay development stage can be performed in buffer (Phase B, Figure 5) and easily translated into whole serum. Finally, the protein immunoassay should be performed in buffer and serum samples, with sample incubation times varied to obtain the effective working window offering negligible or minimum matrix interference (Phase C, Figure 5). This integrated analytical approach will enable the accurate quantitation of different proteins in the microfluidic platforms from non-diluted serum samples as shown in this work.

CONCLUSIONS

Human serum samples matrix interference was fully eliminated in three different miniaturized enzymatic immunoassays (a direct mIgG/anti-mIgG, a sandwich human PSA and a sandwich human IL-1 β) by manipulation of antibody surface coverage and sample incubation time. An optimal antibody density, with antibodies presenting optimal binding capacity, is ideal for overcoming the matrix effect. Longer sample incubation can be effective in minimising sample interference for certain capillary immunoassays, as clearly the equilibrium was not affected by the matrix, only the kinetics of binding is slowed down, yet that strategy revealed diameter-dependent. Our results pointed to matrix interference being linked to competition between low affinity interference factor(s) and high affinity antigen and reagents, therefore both sample dilution and incubation time being effective in minimising matrix interference in microcapillary immunoassays. The novel simple, analytical immunoassay development approach proposed is expected to help speeding up the development of robust, accurate, high-performance and decentralised protein immunoassays. The results shown were specific to fluoropolymer microcapillaries (which allow production of hundreds or thousands of disposable test strips at minimum cost without any complex automation), yet the surface properties of Teflon FEP is not so distinct from other polymers such as PDMS (both hydrophobic) therefore we believe these new bioanalytical approach can benefit the whole community work on immunoassays miniaturisation including conventional and modern microfluidic technologies for POC testing.

AUTHOR INFORMATION

Corresponding Author

*E-mail: n.m.reis@bath.ac.uk; Tel.: +44(0)1225 383 369.

† Loughborough University.

§ University of Reading

‡ University of Bath.

Capillary Film Technology Ltd

Conflict of Interest Disclosure

A. D. Edward and N. M. Reis are co-founders and shareholders of Capillary Film Technology Ltd, a UK-based SME developing fluoropolymer Micro Capillary Film material for advanced uses in life sciences and diagnostics. Also, co-author A. I. Barbosa worked as an employee for Capillary Film Technology Ltd during a period of preparation of this manuscript.

Author Contributions

The manuscript was written through contributions of all authors. All authors have given approval to the final version of the manuscript.

Supporting Information

- Supporting Information Available: The following files are available free of charge.

File name: Supporting information for Barbosa_et_al_ACS Sensors

Brief description of contents: sourcing of MCF material; effect of sample viscosity; kinetics of antibody binding; effect antibody surface coverage; statistical analysis; and image analysis of MCF strips

ACKNOWLEDGEMENT

The authors are grateful to Carina Brandão Dias for experimental assistance with IL-1 β immunoassay in BSA and Patrick Hester from Lamina Dielectrics Ltd for donating the MCF material. A. I. Barbosa is

grateful to Loughborough University for sponsorship of Ph.D. scholarship. A.D. Edwards is grateful EPSRC (grant EP/L013983/1) for funding.

References

- (1) Tate, J.; Ward, G. Interferences in Immunoassay. *Clin. Biochem. Rev.* **2004**, *25* (2), 105–120.
- (2) Leeflang, M. M. G.; Allerberger, F. How to: Evaluate a Diagnostic Test. *Clinical Microbiology and Infection*. Elsevier B.V. January 1, 2019, pp 54–59. <https://doi.org/10.1016/j.cmi.2018.06.011>.
- (3) Barbosa, A. I.; Castanheira, A. P.; Edwards, A. D.; Reis, N. M. A Lab-in-a-Briefcase for Rapid Prostate Specific Antigen (PSA) Screening from Whole Blood. *Lab Chip* **2014**, *14* (16), 2918–2928. <https://doi.org/10.1039/c4lc00464g>.
- (4) Levinson, S. S.; Miller, J. J. Towards a Better Understanding of Heterophile (and the like) Antibody Interference with Modern Immunoassays. *Clin. Chim. Acta.* **2002**, *325* (1–2), 1–15.
- (5) Selby, C. Interference in Immunoassay. *Ann. Clin. Biochem.* **1999**, *36* (Pt 6), 704–721.
- (6) Weber, T. H.; Käpyaho, K. I.; Tanner, P. Endogenous Interference in Immunoassays in Clinical Chemistry. A Review. *Scand. J. Clin. Lab. Invest. Suppl.* **1990**, *201*, 77–82.
- (7) Boscato, L. M.; Stuart, M. C. Incidence and Specificity of Interference in Two-Site Immunoassays. *Clin. Chem.* **1986**, *32* (8), 1491–1495.
- (8) Chiu, M. L.; Lawi, W.; Snyder, S. T.; Wong, P. K.; Liao, J. C.; Gau, V. Matrix Effects-A Challenge Toward Automation of Molecular Analysis. *JALA - J. Assoc. Lab. Autom.* **2010**, *15* (3), 233–242. <https://doi.org/10.1016/j.jala.2010.02.001>.
- (9) Crevillén, A. G.; Hervás, M.; López, M. A.; González, M. C.; Escarpa, A. Real Sample Analysis on Microfluidic Devices. *Talanta*. Elsevier December 15, 2007, pp 342–357. <https://doi.org/10.1016/j.talanta.2007.10.019>.
- (10) Sonker, M.; Sahore, V.; Woolley, A. T. Recent Advances in Microfluidic Sample Preparation and Separation Techniques for Molecular Biomarker Analysis: A Critical Review. *Analytica Chimica Acta*. Elsevier B.V. September 15, 2017, pp 1–11. <https://doi.org/10.1016/j.aca.2017.07.043>.
- (11) Sepetiene, R.; Sidlauskiene, R.; Patamsyte, V. Plasma for Laboratory Diagnostics. In *Plasma Medicine - Concepts and Clinical Applications*; InTech, 2018. <https://doi.org/10.5772/intechopen.76092>.
- (12) Masson, J. F. Consideration of Sample Matrix Effects and “Biological” Noise in Optimizing the Limit of Detection of Biosensors. *ACS sensors*. NLM (Medline) November 25, 2020, pp 3290–3292. <https://doi.org/10.1021/acssensors.0c02254>.
- (13) Barbosa, A. I.; Reis, N. M. A Critical Insight into the Development Pipeline of Microfluidic Immunoassay Devices for the Sensitive Quantitation of Protein Biomarkers at the Point of Care. *Analyst*. 2017, pp 858–882. <https://doi.org/10.1039/c6an02445a>.
- (14) Nayak, S.; Blumenfeld, N. R.; Laksanasopin, T.; Sia, S. K. Point-of-Care Diagnostics: Recent Developments in a Connected Age. *Analytical Chemistry*. American Chemical Society January 3, 2017, pp 102–123. <https://doi.org/10.1021/acs.analchem.6b04630>.
- (15) Mielczarek, W. S.; Obaje, E. A.; Bachmann, T. T.; Kersaudy-Kerhoas, M. Microfluidic Blood Plasma Separation for Medical Diagnostics: Is It Worth It? *Lab Chip* **2016**, *16* (18), 3441–3448. <https://doi.org/10.1039/c6lc00833j>.
- (16) Liu, C.; Liao, S. C.; Song, J.; Mauk, M. G.; Li, X.; Wu, G.; Ge, D.; Greenberg, R. M.; Yang, S.; Bau, H. H. A High-Efficiency Superhydrophobic Plasma Separator. *Lab Chip* **2016**, *16* (3), 553–560. <https://doi.org/10.1039/c5lc01235j>.

- (17) Son, J. H.; Lee, S. H.; Hong, S.; Park, S. M.; Lee, J.; Dickey, A. M.; Lee, L. P. Hemolysis-Free Blood Plasma Separation. *Lab Chip* **2014**, *14* (13), 2287–2292. <https://doi.org/10.1039/c4lc00149d>.
- (18) Yeo, J. C.; Wang, Z.; Lim, C. T. Microfluidic Size Separation of Cells and Particles Using a Swinging Bucket Centrifuge. *Biomicrofluidics* **2015**, *9* (5). <https://doi.org/10.1063/1.4931953>.
- (19) Chen, C. C.; Lin, P. H.; Chung, C. K. Microfluidic Chip for Plasma Separation from Undiluted Human Whole Blood Samples Using Low Voltage Contactless Dielectrophoresis and Capillary Force. *Lab Chip* **2014**, *14* (12), 1996–2001. <https://doi.org/10.1039/c4lc00196f>.
- (20) Kuan, D. H.; Wu, C. C.; Su, W. Y.; Huang, N. T. A Microfluidic Device for Simultaneous Extraction of Plasma, Red Blood Cells, and On-Chip White Blood Cell Trapping. *Sci. Rep.* **2018**, *8* (1), 15345. <https://doi.org/10.1038/s41598-018-33738-8>.
- (21) Tripathi, S.; Kumar, Y. V. B.; Agrawal, A.; Prabhakar, A.; Joshi, S. S. Microdevice for Plasma Separation from Whole Human Blood Using Bio-Physical and Geometrical Effects. *Sci. Rep.* **2016**, *6*, 26749. <https://doi.org/10.1038/srep26749>.
- (22) Tajudin, A. A.; Petersson, K.; Lenshof, A.; Swärd-Nilsson, A. M.; Åberg, L.; Marko-Varga, G.; Malm, J.; Lilja, H.; Laurell, T. Integrated Acoustic Immunoaffinity-Capture (IAI) Platform for Detection of PSA from Whole Blood Samples. *Lab Chip* **2013**, *13* (9), 1790–1796. <https://doi.org/10.1039/c3lc41269e>.
- (23) Browne, A. W.; Ramasamy, L.; Cripe, T. P.; Ahn, C. H. A Lab-on-a-Chip for Rapid Blood Separation and Quantification of Hematocrit and Serum Analytes. *Lab Chip* **2011**, *11* (14), 2440–2446. <https://doi.org/10.1039/c1lc20144a>.
- (24) Svensson, O.; Arnebrant, T. Antibody-Antigen Interaction on Polystyrene: An in Situ Ellipsometric Study. *J. Colloid Interface Sci.* **2012**, *368* (1), 533–539. <https://doi.org/10.1016/j.jcis.2011.11.034>.
- (25) Baleviciute, I.; Balevicius, Z.; Makaraviciute, A.; Ramanaviciene, A.; Ramanavicius, A. Study of Antibody/Antigen Binding Kinetics by Total Internal Reflection Ellipsometry. *Biosens. Bioelectron.* **2013**, *39* (1), 170–176. <https://doi.org/10.1016/j.bios.2012.07.017>.
- (26) Barbosa, A. I.; Gehlot, P.; Sidapra, K.; Edwards, A. D.; Reis, N. M. Portable Smartphone Quantitation of Prostate Specific Antigen (PSA) in a Fluoropolymer Microfluidic Device. *Biosens. Bioelectron.* **2015**, *70*, 5–14. <https://doi.org/10.1016/j.bios.2015.03.006>.
- (27) Sturgeon, C. M.; Viljoen, A. Analytical Error and Interference in Immunoassay: Minimizing Risk. *Annals of Clinical Biochemistry*. SAGE PublicationsSage UK: London, England September 1, 2011, pp 418–432. <https://doi.org/10.1258/acb.2011.011073>.
- (28) Ismail, A. A. A.; Walker, P. L.; Cawood, M. L.; Barth, J. H. Interference in Immunoassay Is an Underestimated Problem. *Annals of Clinical Biochemistry*. 2002, pp 366–373. <https://doi.org/10.1258/000456302760042128>.
- (29) Edwards, A. D.; Reis, N. M.; Slater, N. K. H.; Mackley, M. R. A Simple Device for Multiplex ELISA Made from Melt-Extruded Plastic Microcapillary Film. *Lab Chip* **2011**, *11* (24), 4267–4273. <https://doi.org/10.1039/c0lc00357c>.
- (30) Hallmark, B.; Mackley, M. R.; Gadala-Maria, F. Hollow Microcapillary Arrays in Thin Plastic Films. *Adv. Eng. Mater.* **2005**, *7* (6), 545–547. <https://doi.org/10.1002/adem.200400154>.
- (31) Barbosa, A. I.; Barreto, A. S.; Reis, N. M. Transparent, Hydrophobic Fluorinated Ethylene Propylene Offers Rapid, Robust, and Irreversible Passive Adsorption of Diagnostic Antibodies for Sensitive Optical Biosensing. *ACS Appl. Bio Mater.* **2019**, *2* (7), 2780–2790. <https://doi.org/10.1021/acsabm.9b00214>.
- (32) Castanheira, A. P.; Barbosa, A. I.; Edwards, A. D.; Reis, N. M. Multiplexed Femtomolar Quantitation of Human Cytokines in a Fluoropolymer Microcapillary Film. *Analyst* **2015**, *140* (16), 5609–5618. <https://doi.org/10.1039/c5an00238a>.
- (33) Schneider, C. A.; Rasband, W. S.; Eliceiri, K. W. NIH Image to ImageJ: 25 Years of Image Analysis.

Nat. Methods **2012**, 9 (7), 671–675. <https://doi.org/10.1038/nmeth.2089>.

- (34) Zimmermann, M.; Delamarche, E.; Wolf, M.; Hunziker, P. Modeling and Optimization of High-Sensitivity, Low-Volume Microfluidic-Based Surface Immunoassays. *Biomed. Microdevices* **2005**, 7 (2), 99–110. <https://doi.org/10.1007/s10544-005-1587-y>.
- (35) Barbosa, A. I.; Castanheira, A. P.; Reis, N. M. Sensitive Optical Detection of Clinically Relevant Biomarkers in Affordable Microfluidic Devices: Overcoming Substrate Diffusion Limitations. *Sensors Actuators B Chem.* **2018**, 258, 313–320. <https://doi.org/10.1016/J.SNB.2017.11.086>.
- (36) Wu, F. B.; He, Y. F.; Han, S. Q. Matrix Interference in Serum Total Thyroxin (T4) Time-Resolved Fluorescence Immunoassay (TRFIA) and Its Elimination with the Use of Streptavidin-Biotin Separation Technique. *Clin. Chim. Acta.* **2001**, 308 (1–2), 117–126.
- (37) Sauer, U.; Pultar, J.; Preininger, C. Critical Role of the Sample Matrix in a Point-of-Care Protein Chip for Sepsis. *J. Immunol. Methods* **2012**, 378 (1–2), 44–50. <https://doi.org/10.1016/j.jim.2012.02.002>.
- (38) Taylor, T. P.; Janech, M. G.; Slate, E. H.; Lewis, E. C.; Arthur, J. M.; Oates, J. C. Overcoming the Effects of Matrix Interference in the Measurement of Urine Protein Analytes. *Biomark. Insights* **2012**, 7, 1–8. <https://doi.org/10.4137/BMI.S8703>.
- (39) The Stokes-Einstein Law for Diffusion in Solution. *Proc. R. Soc. London. Ser. A, Contain. Pap. a Math. Phys. Character* **1924**, 106 (740), 724–749. <https://doi.org/10.1098/rspa.1924.0100>.
- (40) Hadzhieva, M.; Pashov, A. D.; Kaveri, S.; Lacroix-Desmazes, S.; Mouquet, H.; Dimitrov, J. D. Impact of Antigen Density on the Binding Mechanism of IgG Antibodies. *Sci. Rep.* **2017**, 7 (1), 1–11. <https://doi.org/10.1038/s41598-017-03942-z>.

AS accepted

List of tables

Table 1 - IL-1 β sandwich assay sensitivity considerations in buffer and in human serum after 4PL model fitting and analyses (Figures 3 C and D)

Sample Incubation Time (min)	Sample matrix	Lower Limit of Detection (LLoD) ng/ml	Precision (with 0.125 ng/ml IL-1 β)	R ² (with 4PL model)
5	buffer	0.021	9%	0.9992
5	100% serum	0.014	6%	0.9989
5	50% serum	0.006	19%	0.9991
30	buffer	0.084	20%	0.9929
30	100% serum	0.051	10%	0.9965

Table 2 - Kinetic constants of anti-mIgG binding in buffer and human serum in different capillary diameter MCF (Figures 4 C and D).

	Buffer			Human serum		
	109 μ m MCF	212 μ m MCF	375 μ m MCF	109 μ m MCF	212 μ m MCF	375 μ m MCF
K_{on} (M s ⁻¹)	6.39 x 10 ⁶	4.24 x 10 ⁶	2.65 x 10 ⁶	5.38 x 10 ⁶	3.35 x 10 ⁶	9.62 x 10 ⁷
K_{off} (s ⁻¹)	1.42 x 10 ⁻³	1.71 x 10 ⁻³	1.55 x 10 ⁻³	8.52 x 10 ⁻³	1.91 x 10 ⁻³	4.13 x 10 ⁻²
Kd (M ⁻¹)	2.23 x 10 ⁻¹⁰	4.04 x 10 ⁻¹⁰	5.87 x 10 ⁻¹⁰	1.58 x 10 ⁻⁹	5.70 x 10 ⁻¹⁰	4.29 x 10 ⁻¹⁰

Figures captions

Figure 1. Human serum matrix effect in MCF diagnostic strips. A MCF and the fluid handling set-up for diagnostic procedures. B PSA sandwich assay full response curves in human serum and buffer, showing the matrix effect interference. C Schematic of the capillary immunoassays in the MCF platform.

Figure 2. Effect of antibody surface coverage in the matrix effect of human serum of three different MCF protein assays. A Effect of human serum on anti-mIgG detection using a range of 0-200 $\mu\text{g/ml}$ of capture antibody loading. Antigen concentration was kept constant, anti-mIgG = 0.6 $\mu\text{g/ml}$. B Effect of human serum on IL-1 β detection using a range of 0-200 $\mu\text{g/ml}$ of capture antibody loading. Antigen concentration was kept constant, IL-1 β = 0.13 ng/ml. C Effect of human serum on PSA using a range of 0-200 $\mu\text{g/ml}$ of capture antibody loading. Antigen concentration was kept constant, PSA = 3.75 ng/ml. (i) Assay schematics; (ii) Shows the assay signal in buffer and serum, while (ii) shows the ratio of the two signals. The red dash line indicates the limit of 20% variation above which the variability is not acceptable for immunoassay performance.

Figure 3. Effect of sample incubation time in IL-1 β sandwich MCF immunoassays. A IL-1 β sandwich assay in buffer, whole blood and serum, considering 5 minutes sample incubation time, and 0.125 ng/ml of IL-1 β . B IL-1 β sandwich assay in buffer, whole blood and serum, considering 30 minutes sample incubation time and 0.125 ng/ml of IL-1 β . C MCF IL-1 β full response curve using buffer, to 50% and 100% of human serum as sample diluents. The sample was incubated for 5 min. D MCF IL-1 β full response curve using buffer, and 100% of human serum as sample diluents. The sample was incubated for 30 min. All MCF assays were performed using 40 $\mu\text{g/ml}$ of CapAb, which promotes approximately half of immobilized antibody monolayer with antibodies oriented “end-on” with F(ab) in line.³¹ Note that * $P \leq 0.05$; ** $P \leq 0.01$; *** $P \leq 0.001$ in the Tukey's multiple comparisons test.

Figure 4. Relationship between human serum matrix effect and capillary geometry in MCF assays. A (i) Photograph of 3 different MCFs with of 109 \pm 12 μm , 212 \pm 16 μm , 375 \pm 29 μm mean diameter bore. (ii) Microscope photograph of a cross section from the MCFs with 109, 212, 375 μm diameter bore. B The effect of diameter size on total surface area (SA) and on surface-area-to-volume ratio (SAV). C mIgG-anti-mIgG binding kinetics on different diameter MCFs in buffer matrix. D mIgG-anti-mIgG binding kinetics in different diameter MCFs in undiluted human serum matrix.

Figure 5. Analytical approach for minimizing biological matrix interference in MCF sandwich assays. A Diagram with CapAb concentration and sample incubation time for minimizing matrix interference in MCF assays. B Diagram showing MCF assay development and optimization for rapid, sensitive and accurate quantitative assays.

As accepted

List of figures

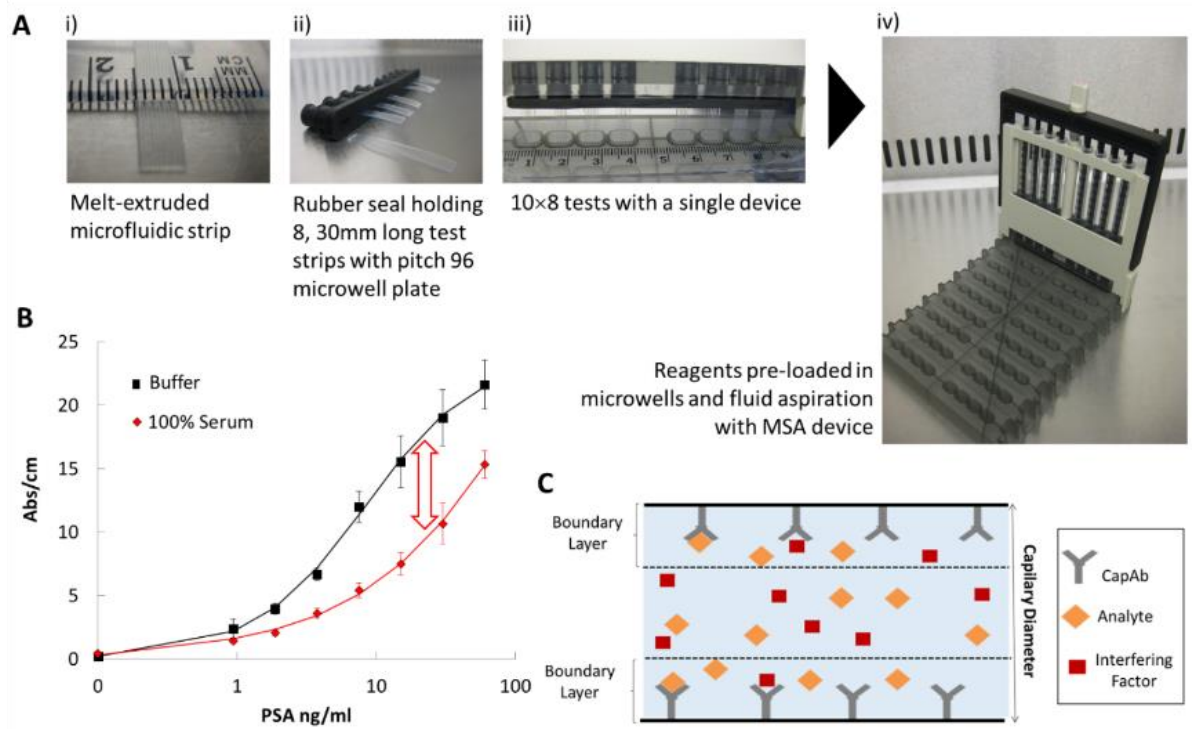


Figure 1

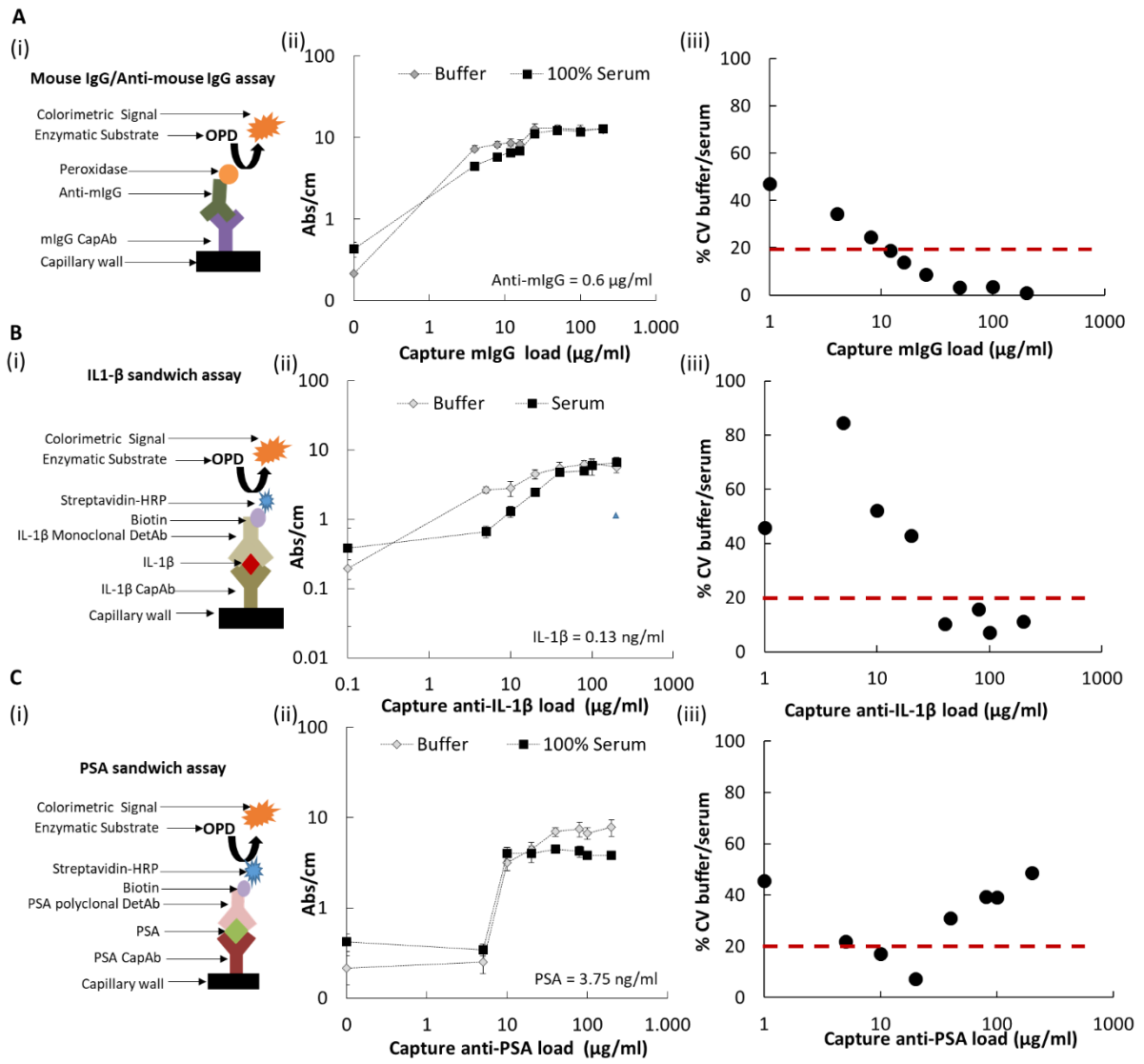


Figure 2

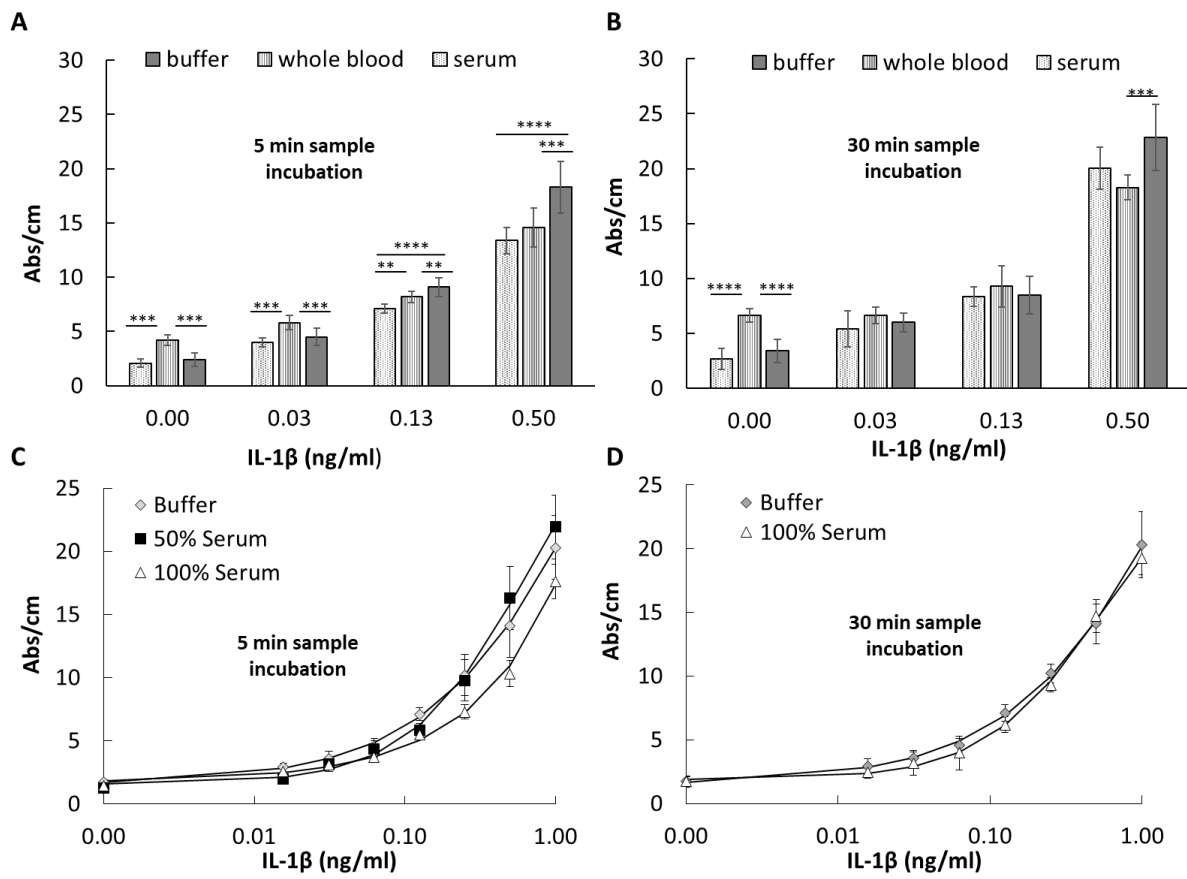


Figure 3

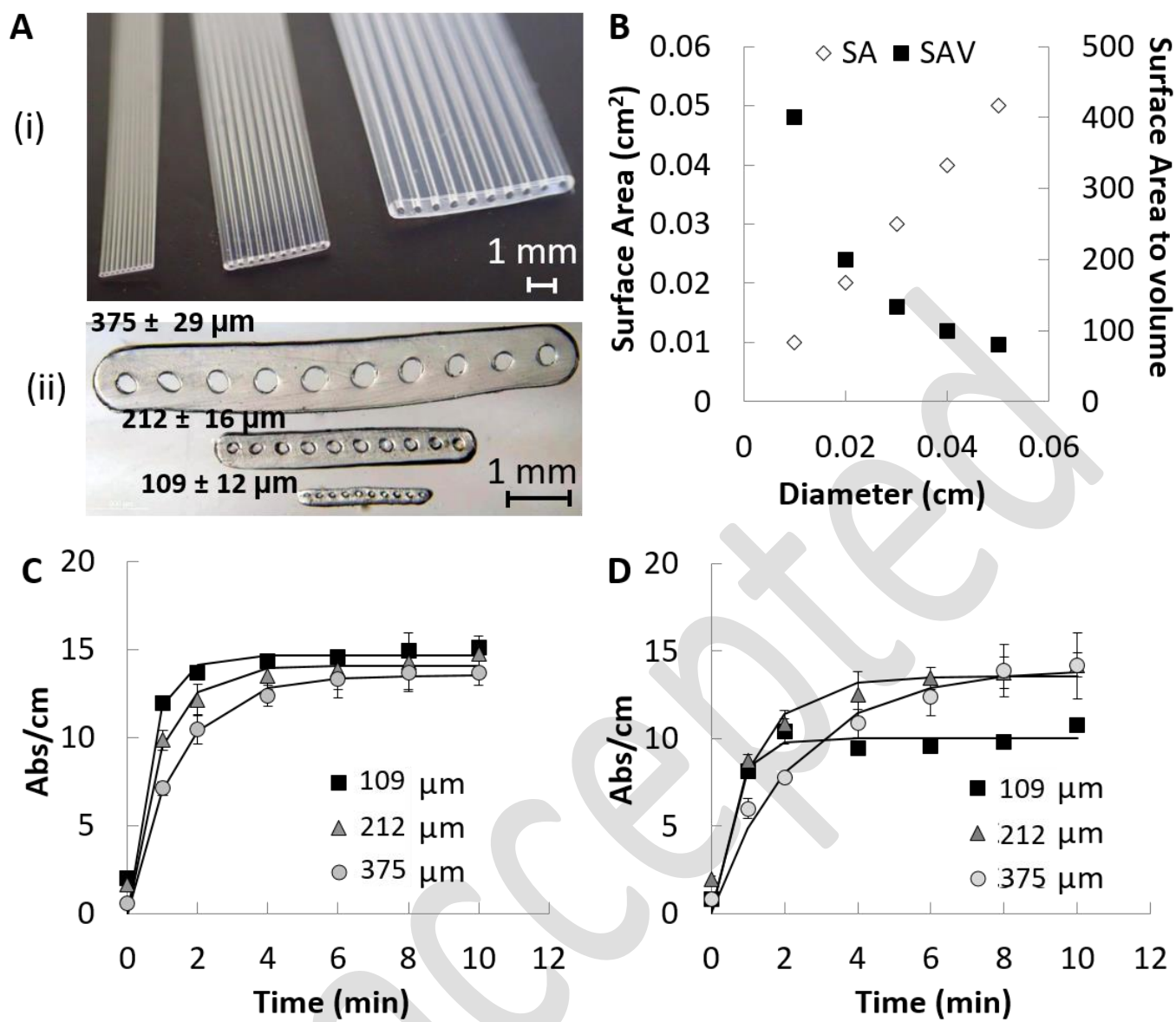


Figure 4

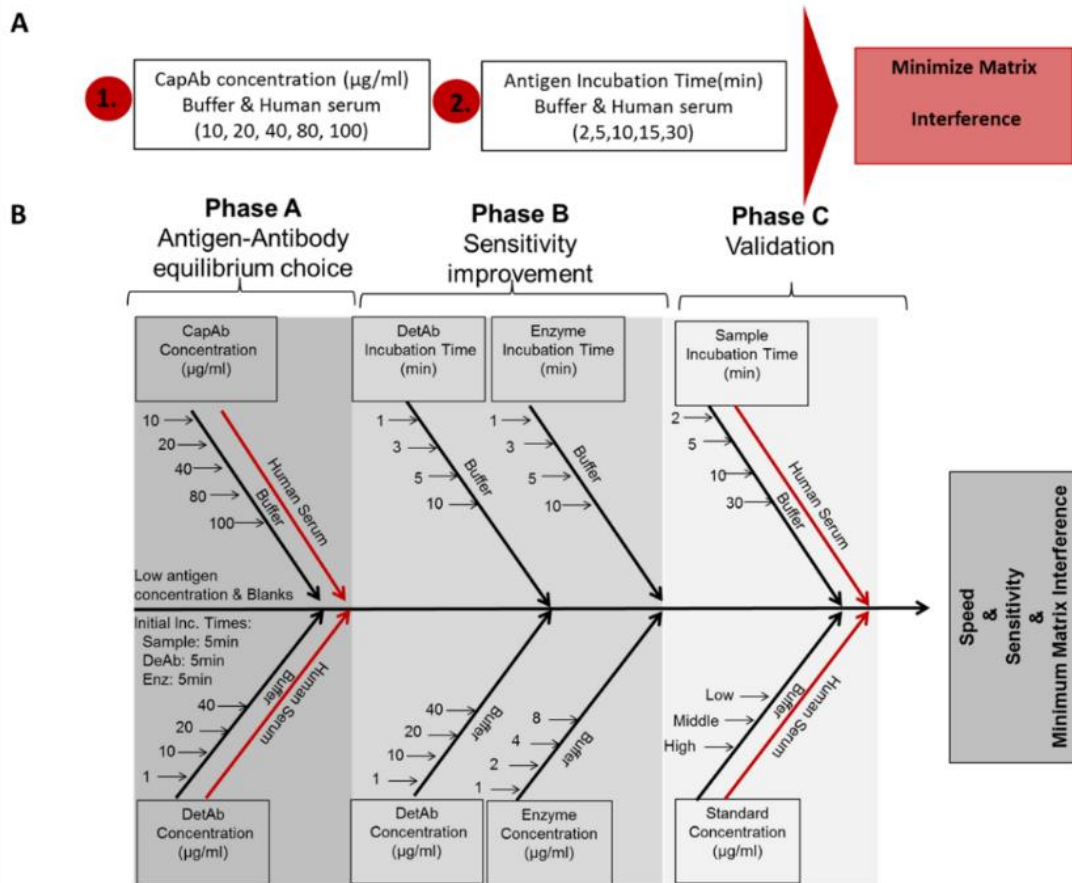
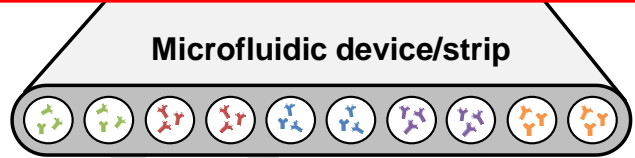
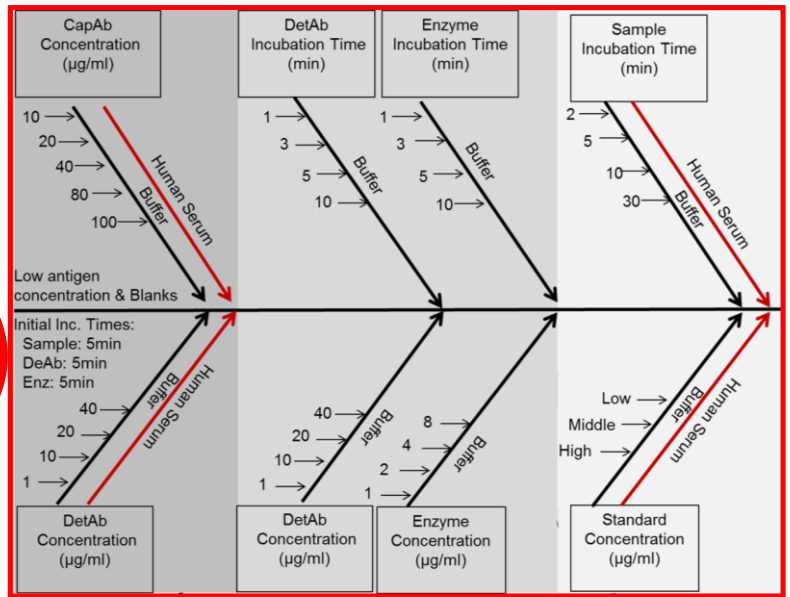
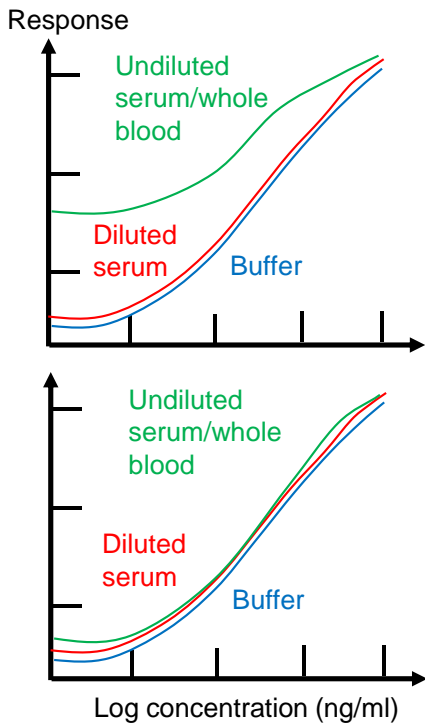


Figure 5

For Table of Contents Only



AS accepted